

XIII Workshop on HIC
Wrocław, Jan 6, 2018

New results on strangeness production from the NA61/SHINE

Maciej Lewicki
mlewicki@ift.uni.wroc.pl

University of Wrocław
Institute of Theoretical Physics



Uniwersytet
Wrocławski

Section 1

Strangeness in Heavy Ion Collisions

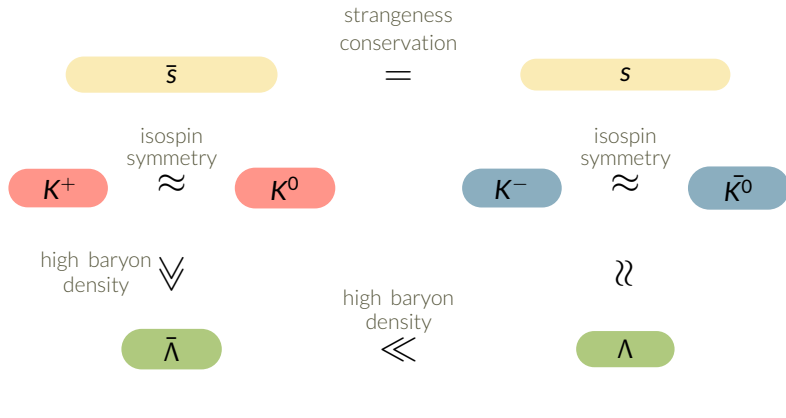
Strangeness in HIC

Most strangeness produced in the form of:

- The lightest (anti-)strange mesons ($M \approx 0.5$ GeV):
 - ▶ $K^+ - (u\bar{s})$
 - ▶ $K^0 - (d\bar{s})$
 - ▶ $K^- - (\bar{u}s)$
 - ▶ $\bar{K}^0 - (\bar{d}s)$
- The lightest (anti-)strange baryons ($M \approx 1.1$ GeV):
 - ▶ $\Lambda - (uds)$
 - ▶ $\bar{\Lambda} - (\bar{u}\bar{d}\bar{s})$
- Strangeness neutral mesons: ($M \approx 1.0$ GeV):
 - ▶ $\phi - (s\bar{s})$

Main strangeness carriers

in A+A collisions at high baryon density



- sensitive to strangeness content only

- sensitive to strangeness content and baryon density

Strange definitions

Strangeness production:

$\langle N_{s\bar{s}} \rangle$ – number of $s\bar{s}$ pairs produced in a collision.

The experimental ratio:

$$E_S = \frac{\langle \Lambda \rangle + \langle K + \bar{K} \rangle}{\langle \pi \rangle} \approx \frac{2 \cdot \langle N_{s\bar{s}} \rangle}{\langle \pi \rangle}$$

$$\langle N_{s\bar{s}} \rangle \approx \langle K^+ \rangle + \langle K^0 \rangle \approx 2 \cdot \langle K^+ \rangle, \quad \langle \pi \rangle \approx \frac{3}{2} (\langle \pi^+ \rangle + \langle \pi^- \rangle)$$

$$\frac{\langle N_{s\bar{s}} \rangle}{\langle \pi \rangle} \approx \frac{2}{3} \frac{\langle K^+ \rangle}{\langle \pi^+ \rangle}$$

$$E_S \approx \frac{4}{3} \frac{\langle K^+ \rangle}{\langle \pi^+ \rangle}$$

It is convenient to study the ratio E_S in this form, as the identification of charged hadrons is relatively easy.

Section 2

Strangeness and Phase Transition

Strangeness and phase transition

confined matter

K mesons

$$g_K = 4$$

$$2M \approx 2 \cdot 500 \text{ MeV}$$

$$T_c \approx 150 \text{ MeV}$$



Phase transition

quark-gluon plasma

(anti-)strange quarks

$$g_s = 12$$

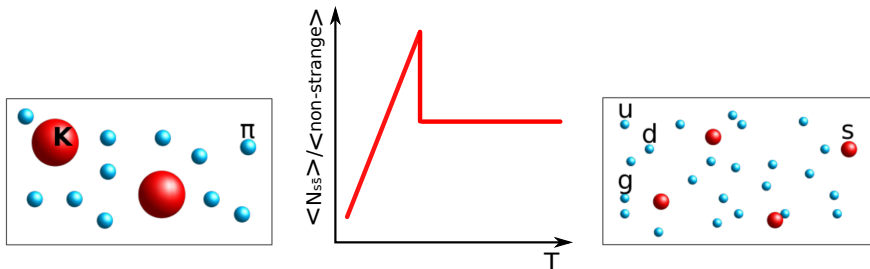
$$2m \approx 2 \cdot 100 \text{ MeV}$$

Lightest strangeness carriers:

- relatively heavy kaons ($M > T_c$) in the confined phase,
- relatively light strange quarks ($m \lesssim T_c$) in QGP.

Strangeness in Statistical Model of Early Stage

$$\langle n \rangle = \frac{gV}{(2\pi)^3} \int d^3p \frac{1}{e^{E/T} \pm 1} \approx gV \left(\frac{MT}{2\pi}\right)^{3/2} e^{-M/T} \quad \text{for heavy particles}$$
$$\approx gV \frac{2\pi^2}{4.45} T^3 \quad \text{for light particles}$$



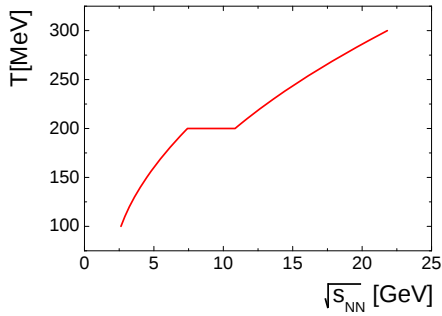
$$\frac{\langle K \rangle}{\langle \pi \rangle} \propto \frac{MT^{3/2}}{T^3} \cdot e^{-M/T}$$

$$\frac{\langle s \rangle}{\langle u + d + g \rangle} \propto \frac{T^3}{T^3} = \text{const}(T)$$

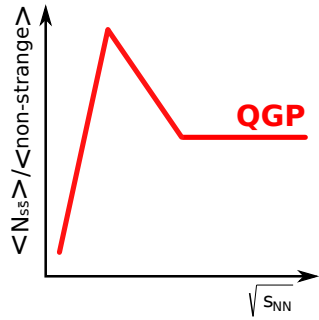
Gaździcki, Gorenstein, Acta Phys. Polon. B30 (1999) 2705

Strangeness in Statistical Model of Early Stage

Temperature dependence
on collision energy in **SMES**:



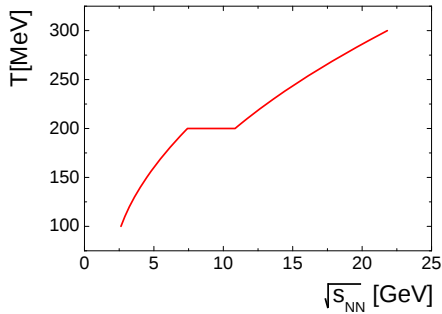
Strange/non-strange
particle ratio:



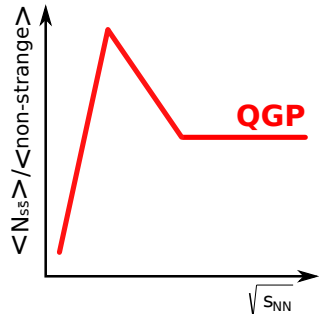
- Crossing the phase transition leads to a decrease of the strange/non-strange particle ratio – the horn-like structure

Strangeness in Statistical Model of Early Stage

Temperature dependence
on collision energy in **SMES**:



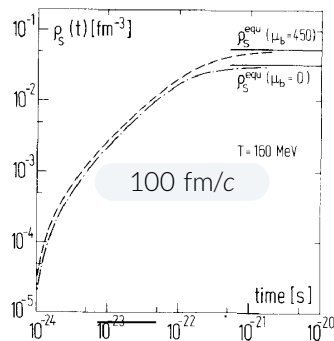
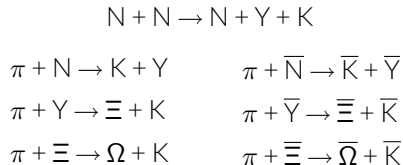
Strange/non-strange
particle ratio:



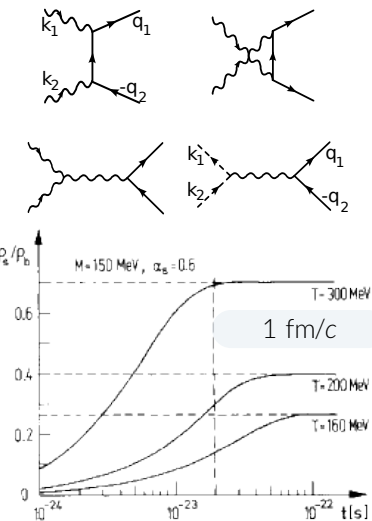
- Crossing the phase transition leads to a decrease of the strange/non-strange particle ratio – the horn-like structure – Marek's horn.

Dynamical Approach by Rafelski-Müller

strangeness production in confined matter

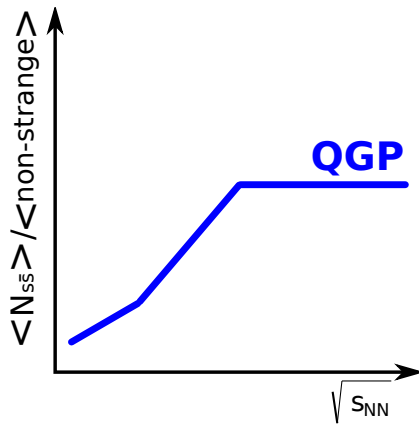


strangeness production in QGP



Rafelski, Müller, Phys. Rev. Lett. 48 (1982) 1066

Rafelski-Müller Dynamical Approach

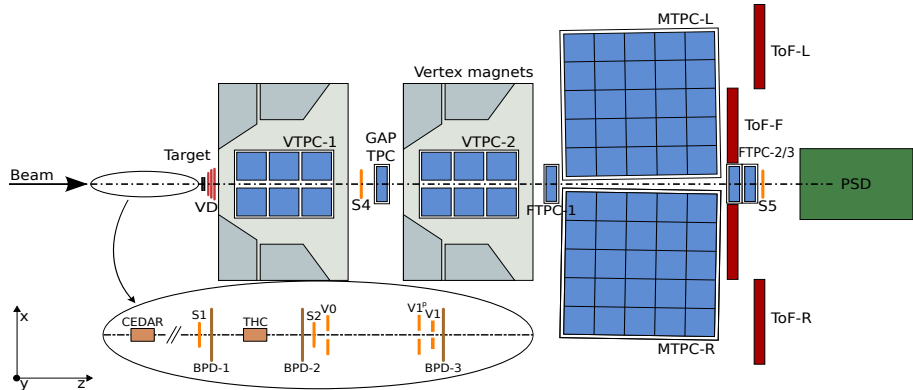


- Equilibrium value reached in QGP ← fast strangeness production.
- No enhancement in the confined phase ← slow strangeness production in whole hadronic region.

Section 3

Strangeness at NA61/SHINE

NA61/SHINE – facility



Beam detectors:

- position
- charge
- mass
- time

TPCs:

- electric charge
- momentum
- dE/dx

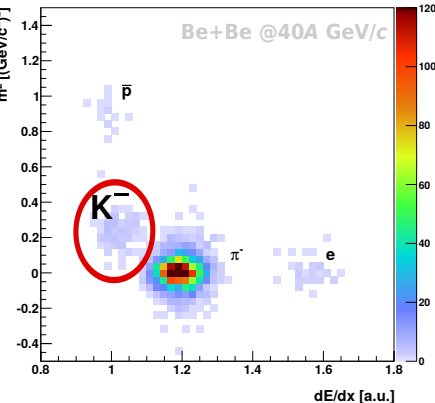
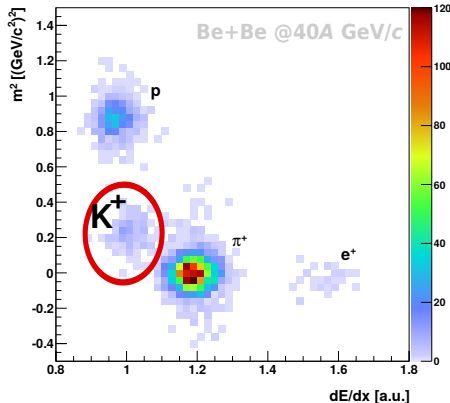
ToF:

- *tof*

PSD:

- E_F – energy of projectile spectators
- reaction plane

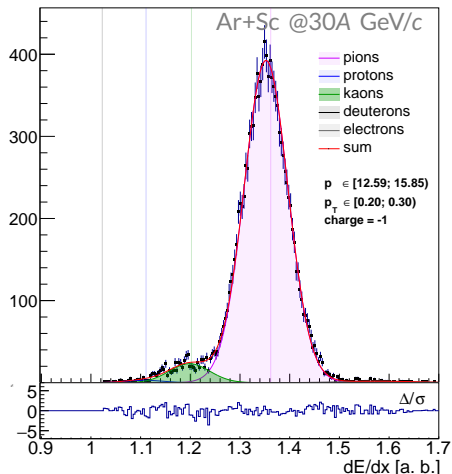
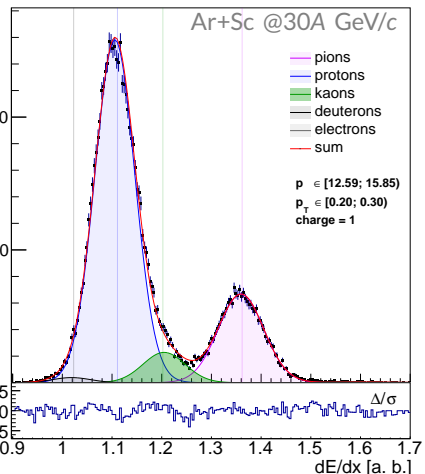
Particle identification – $tof-dE/dx$



Very good separation.

Very efficient PID in mid-rapidity region.

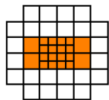
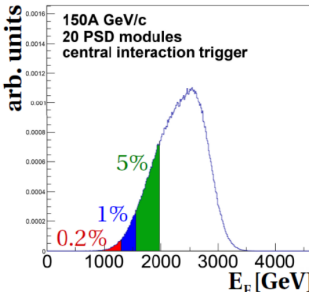
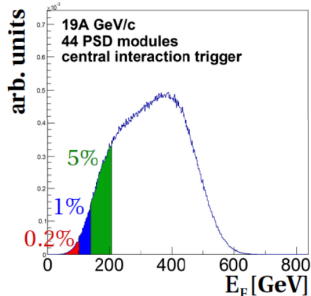
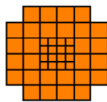
Particle identification – dE/dx



Probability PID.

Applicable in forward-rapidity region.

Event selection



- The PSD is located most downstream on the beam line and measures the projectile spectator energy E_F of the non-interacting nucleons of the beam nucleus.
- The energy measured by the PSD is used to select events classes corresponding to the collision "violence" (\approx centrality).



Section 4

Results on Strangeness

Results on strangeness production

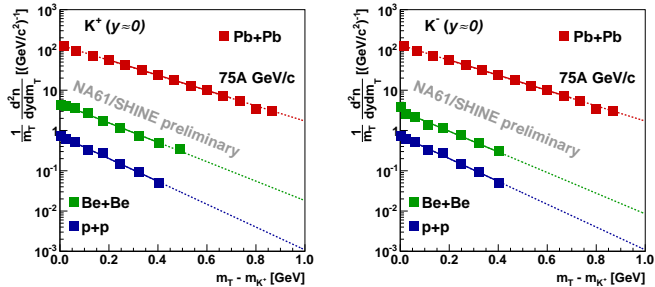
Results from **NA61/SHINE** on identified hadrons produced in strong and electromagnetic processes in primary interactions:

- **Ar+Sc** [CPOD 2017, arXiv:1712.02417]
- **Be+Be** [Nucl. Phys. A 967, 35 (2017)]
- **p+p** [Eur. Phys. J. C74 (2014) 2794, Eur. Phys. J. C77 (2017) 671]

World data on **Pb+Pb**, **Au+Au**, **C+C**, **Si+Si** and **p+p**:

- **NA49**
[Phys. Rev. C77, 024903 (2008)], [Phys. Rev. C66 (2002) 054902], [Phys. Rev. C86 (2012) 054903] [Eur. Phys. J. C68 (2010) 1], [Eur. Phys. J. C45 (2006) 343]
- **ALICE**
[Phys. Lett. B736 (2014) 196], [Eur. Phys. J. C71 (2011) 1655], [Phys. Rev. Lett. (2012) 109]
- **STAR** [Phys. Rev. C79 (2009) 034909], [Phys. Rev. C96 (2017) 044904]
- **BRAHMS** [Phys. Rev. C72 (2005) 014908]
- **p+p world data** [Z. Phys. C65 (1995) 215], [Phys. Rev. C69 (2004) 044903]

m_T spectra and inverse slope parameter



- m_T spectra at mid-rapidity fitted with an exponential function

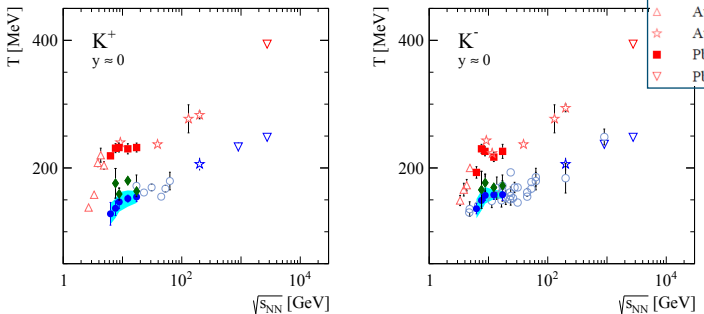
$$\frac{1}{m_T} \frac{d^2n}{dm_T dy} = A \exp\left(-\frac{m_T}{T}\right)$$

which well describes K spectra for all beam momenta and all reactions

- The energy dependence of the inverse slope parameter T was predicted to be sensitive to the phase transition between confined matter and QGP.

Inverse slope parameter

"step" plot

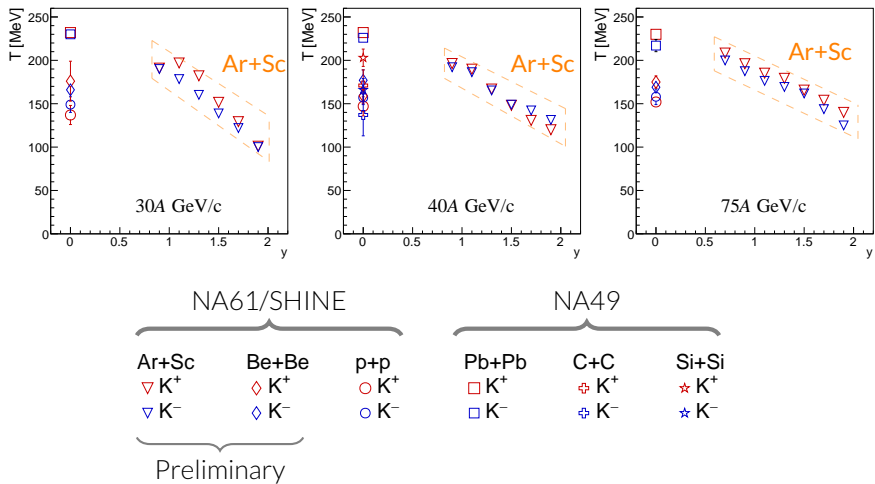


Inverse slope parameter T (vague temperature analogy) – a parameter in fit to transverse mass spectra: $\frac{dn}{m_T dm_T} \cong A \exp\left(-\frac{m_T}{T}\right)$

- A plateau in the phase transition region ($\sqrt{s_{NN}} \approx 10$ GeV) ← predicted by **SMES**.
- **Be+Be** points slightly above **p+p** and both significantly lower than **heavy ions**.

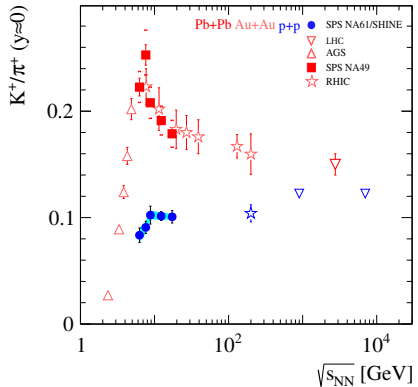
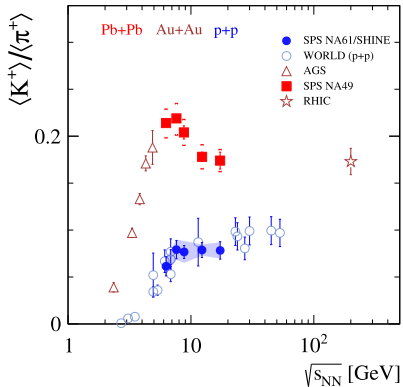
Inverse slope parameter

Extrapolation of Ar+Sc points to $T(y \approx 0)$ falls close to Pb+Pb,
while smaller systems show significantly smaller values.



Energy dependence

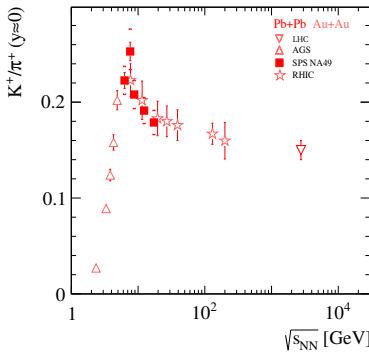
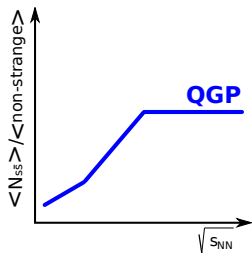
"horn" plot



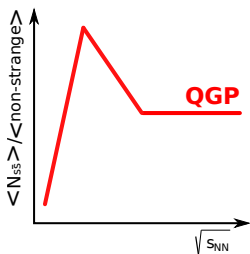
- Rapid change in strangeness production observed in **Pb+Pb** – the horn.
- Plateau-like energy dependence in **p+p** data.

Collision energy dependence of strangeness production

Rafelski-Müller



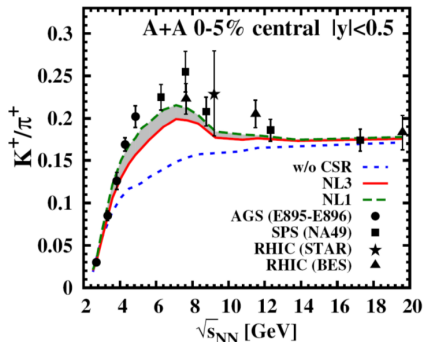
SMES



- Qualitatively, **heavy-ion** data follows dependence predicted by **SMES**.
- The dependence predicted by the **Rafelski-Müller** model is in contradiction with **heavy-ion** data.

PHSD model with & without Chiral Symmetry Restoration

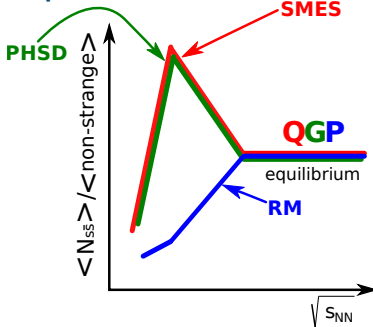
in the confined phase



- Without CSR – prediction of PHSD qualitatively resembles predictions of the Rafelski-Müller model.
- With CSR – enhanced strangeness production in the confined phase.
The strange quark mass used in the string decay Schwinger-formula is assumed to decrease with energy density, while still in the confined phase.

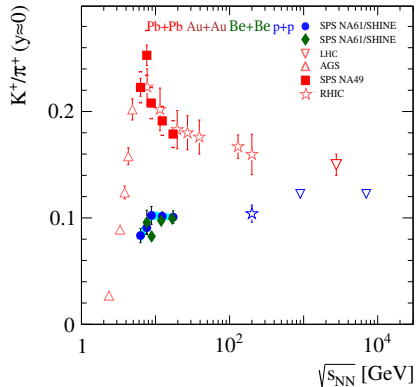
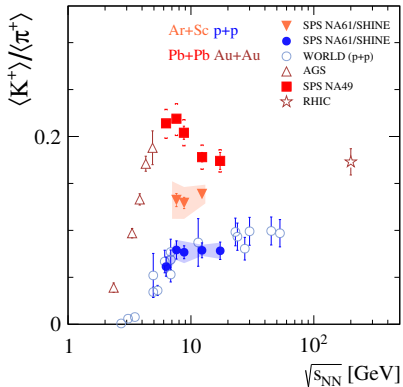
Palmese et al., PRC94 (2016) 044912

Summary – Model predictions with transition to QGP



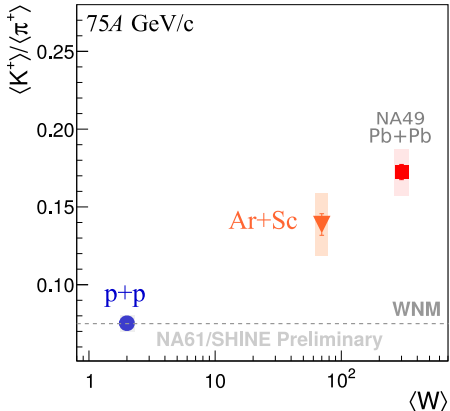
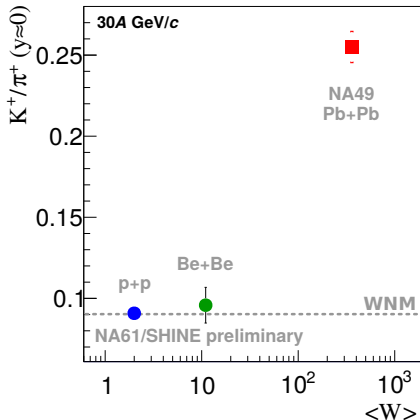
- High energies – all three models with phase transition predict the strange/non-strange particle ratio close to the one for the equilibrium QGP.
- At low collision energies (in the confined matter):
 - ▶ RM model predicts: a) large equilibration time,
b) insignificant strangeness enhancement wrt. initial state.
 - ▶ PHSD cures this problem reducing the strange quark mass in string decays.
 - ▶ SMES overcomes it by postulating the statistical particle production at early stage of collisions.

System size dependence of strangeness production



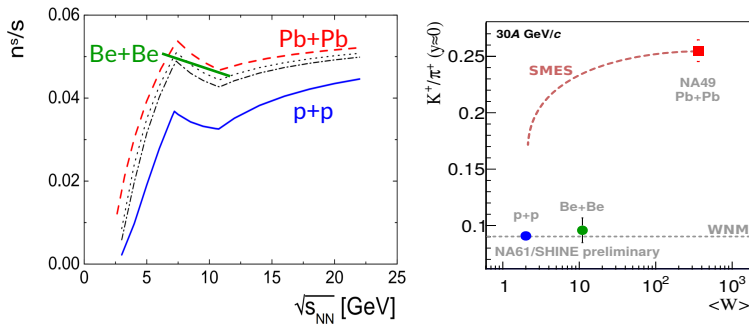
- Ar+Sc placed in between light and heavy systems.
- Be+Be very close to p+p.

System size dependence



- Be+Be resembles closely the p+p data.
- Similar behavior at all energies and in the measurement of fluctuations.
- → Another threshold of collisions dynamics – **onset of fireball**.
- Ar+Sc much closer to Pb+Pb

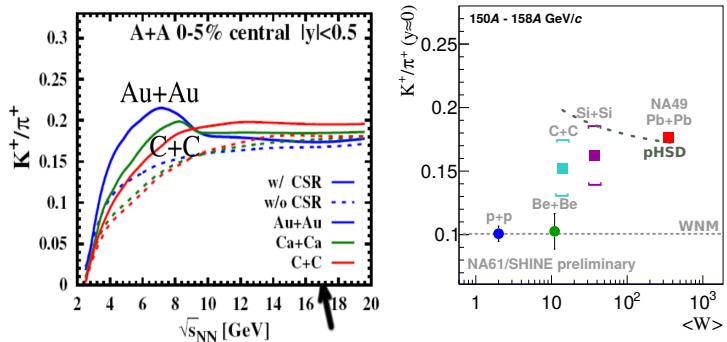
System size dependence of strangeness production - SMES



- SMES predicts very different system size dependence of K^+/π^+ ratio than the one measured by the NA61/SHINE experiment.
- System size dependence predicted by SMES is due to diminishing effect of the canonical strangeness suppression with increasing volume within statistical models.

Poberezhnyuk, Gaździcki, Gorenstein, Acta Phys. Polon. B46 (2015) 10

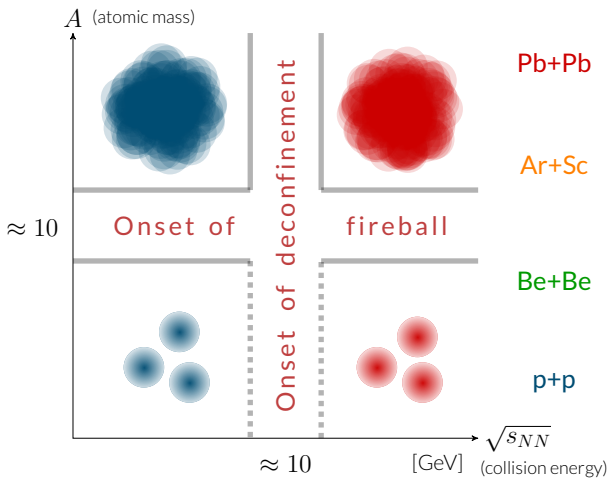
System size dependence of strangeness production - PHSD



- PHSD predicts increase of strangeness production with system size at low collision energies (<10 GeV) and decrease at high collision energies (>10 GeV).
- PHSD predictions in disagreement with data at high energies.

Palmese et al., PRC94 (2016) 044912

The Two Onsets



- **Onset of deconfinement:**
beginning of creation of QGP with increasing collision energy ($\sqrt{s_{NN}}$).
- **Onset of fireball:**
beginning of creation of large clusters of strongly interacting mater in A+A collisions with increasing nuclear mass number (A).

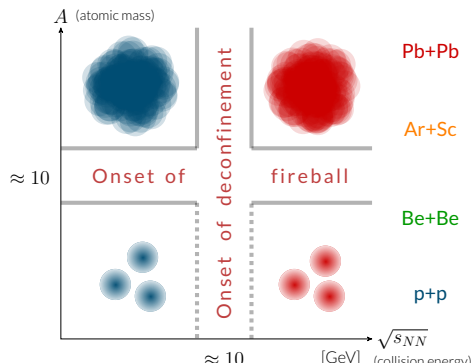
Summary

- 1 Models of strangeness production in phase transition were reviewed. Dynamical and statistical approaches were compared.
- 2 NA61/SHINE's results on $p+p$, $Be+Be$ (preliminary) and $Ar+Sc$ (preliminary) were presented:
 - ▶ transverse mass m_T spectra of kaons and inverse slope parameter T ,
 - ▶ mean multiplicities of kaons.
- 3 Energy dependence of strangeness production in **light** and **heavy** systems was reviewed.
- 4 Clear qualitative difference between light ($p+p$, $Be+Be$) and heavy ($Ar+Sc$, $Pb+Pb$) systems measurements observed.
- 5 It was found that none of existing models can reproduce measured system size dependence.
- 6 Two threshold behaviors (onsets) were observed: the onset of deconfinement and the onset of fireball.

Thank you for your attention!

BACKUP SLIDES

The Two Onsets



- **Percolation approach:**

Increasing nuclear mass \rightarrow density of clusters (strings, partons...) increases

\rightarrow Probability of cluster overlapping increases.

\rightarrow Conservation laws act on the whole cluster.

This approach does not explain equilibrium properties of large clusters.

Physica A96 (1979) 131-135; Phys. Lett. B97 (1980) 128-130; Nucl. Phys. B390 (1993) 542-558; Phys. Rev.

Lett 77 (1996) 3736-3738; Phys. Rev. C72 (2005) 024907

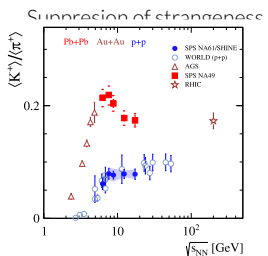
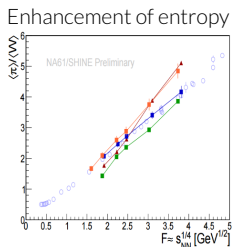
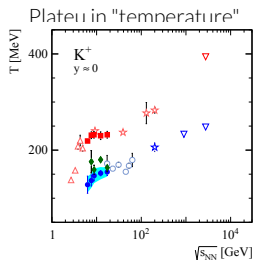
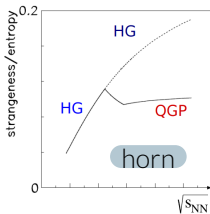
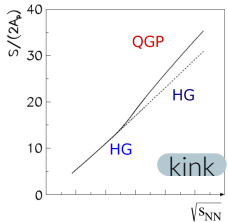
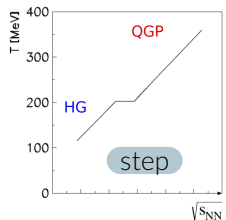
- **AdS/CFT correspondence:**

AdS (gravity) - formation of a black hole horizon, the information trapping takes place when critical values of model parameters are reached.

CFT (QCD) - only starting from a sufficiently large nuclear mass number the formation of the trapping surface in A+A collisions is possible.

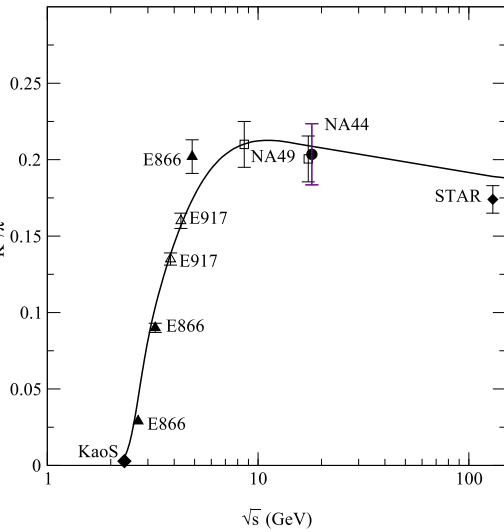
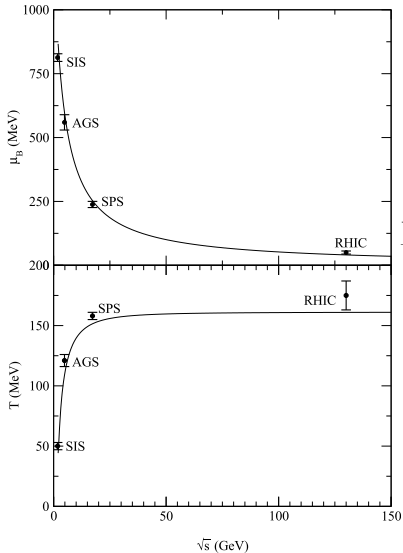
Prog. Part. Nucl. Phys. (2009) 62; Phys. Rev. D79 (2009) 124015

Predictions of SMES



Experimental results – confirming SMES predictions.
Signatures of PT happen all at the same $\sqrt{s_{NN}}$.

Predictions of Hadron Resonance Gas model



[Nucl.Phys. A697 (2002) 902-912]

Results stand for primary particles produced in strong and electromagnetic processes.

Corrections:

- Results are corrected for:
 - ▶ biases in event selection
 - ▶ reconstruction inefficiency
 - ▶ weak decays
 - ▶ secondary interactions
 - ▶ detector geometrical acceptance.
- MC used for corrections: EPOS 1.99 model and GEANT3.2+NA61/SHINE detector simulation.

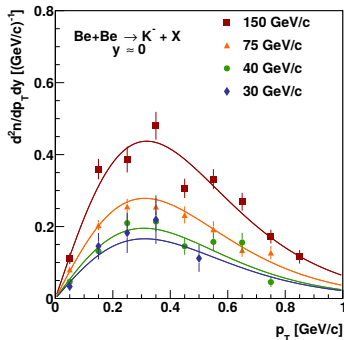
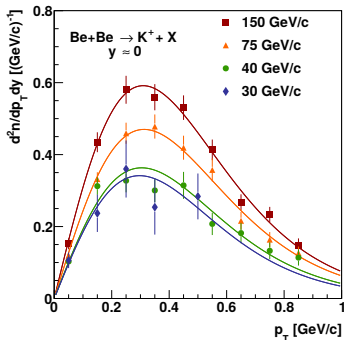
Uncertainties:

- There are two sources of statistical uncertainties in results:
 - ▶ data uncertainties
 - ▶ MC corrections uncertainties (insignificant).
- The systematic uncertainties comes from:
 - ▶ limited precision of simulation and detector description.

For nucleus-nucleus collisions, the event classes are defined by forward energy measured by PSD. Results for p+p collisions refer to all inelastic interactions.

Particle yield extrapolation to full p_T acceptance

Examples for Be+Be



- In order to obtain the dn/dy yields of K mesons, the data is extrapolated with the exponential function in m_T beyond the detector acceptance.
- $dn/(dp_T dy)$ spectra were fitted with the corresponding function in p_T .
- The function integral outside the acceptance region (<10%) is added to the measured yield.

Fitting rapidity distribution

Two symmetrically placed gaussians are used to construct the fitting function:

$$f_{\text{fit}}(y) = \frac{A}{\sigma_0 \sqrt{2\pi}} \exp\left(-\frac{(y - y_0)^2}{2\sigma_0^2}\right) + \frac{A}{\sigma_0 \sqrt{2\pi}} \exp\left(-\frac{(y + y_0)^2}{2\sigma_0^2}\right)$$

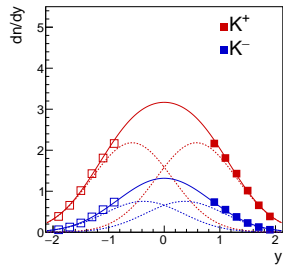
Shape parameters: y_0 and σ are fixed to values obtained in NA49's Pb+Pb.

The amplitude A is the only free parameter.

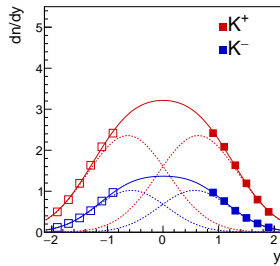
Varying the shape parameters provides an estimate of a systematic error.

Rapidity Distribution

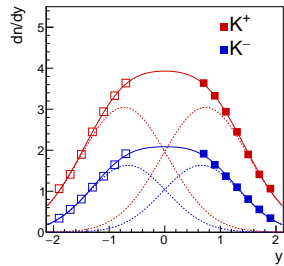
30A GeV/c



40A GeV/c



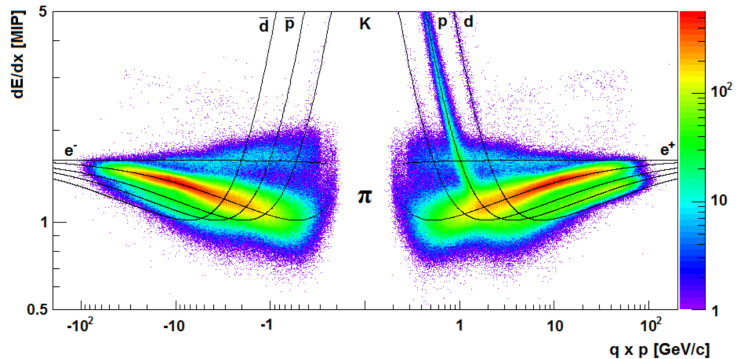
75A GeV/c



Pb+Pb spectra shape fits Ar+Sc data surprisingly well.

Measurements of tof will add data in $y \approx 0$ region in the near future.

dE/dx distribution



Functions are fitted to experimental data by considering the parameters depending on the absorbing material as free fit parameters:

$$\left\langle -\frac{dE}{dx} \right\rangle_{trunc} = E_0 \frac{1}{\beta^2} (K + \ln(\gamma) - \beta^2 - \delta(\beta, X_A, a))$$

E_0 contains all the constant factors.

K adjusts for the shape of the curve around the minimum.

Parameters fitted to the data: E_0 , K , X_A , a

Truncated mean $\langle dE/dx \rangle_{Tr}$ distribution

The basic peak shape is assumed to be a sum of asymmetric Gaussians:

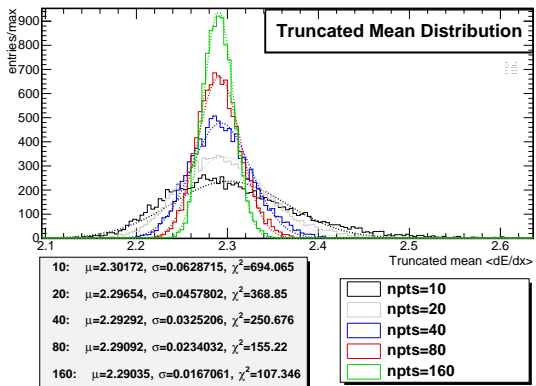
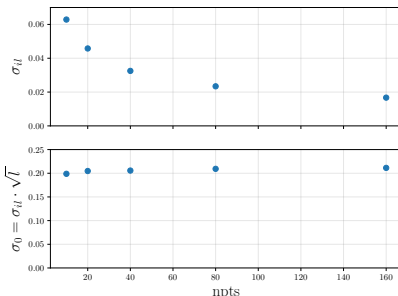
$$\left\langle \frac{dE}{dx} \right\rangle_{total} = \sum_{i=d,p,K,\pi,e} N_i \frac{1}{\sum_I n_I} \sum_I \frac{n_I}{\sqrt{2\pi}\sigma_{i,I}} \exp \left[-\frac{1}{2} \left(\frac{x - x_i}{(1 \pm \delta)\sigma_{i,I}} \right)^2 \right]$$

with widths $\sigma_{i,I}$

($I \equiv \text{npts} \equiv \# \text{ of clusters}$):

$$\sigma_{i,I} = \frac{\sigma_0}{\sqrt{I}} \left(\frac{x_i}{x_1} \right)^\alpha$$

(I^β arbitrary fixed at $\beta = -\frac{1}{2}$)



Strangeness suppression in Q-state

g_W^s, g_Q^s – numbers of internal dof of (anti)strangeness carriers in W-, Q-state.

The entropy carried by strange (and antistrange) particles:

$$S_s = \frac{g_s}{g} S$$

For massless particles of j -th species:

$$S_j = 4N_j, \quad N_s + N_{\bar{s}} = \frac{S}{4} \frac{g_s}{g}$$

And the strangeness to entropy ratio:

$$\frac{N_s + N_{\bar{s}}}{S} = \frac{1}{4} \frac{g_s}{g}$$

Estimate (for massless dof):

$$\text{Q-state: } g_Q^s/g_Q \approx 0.22, \quad \text{W-state: } g_W^s/g_W \approx 0.5$$

Numerical calculations with true masses considered:

energy dependent